Adsorption of Unsaturated Hydrocarbon Moieties on H:Si(111) by Grignard Reaction

Taro Yamada,[†] Kaoru Shirasaka,[†,‡] Madomi Noto,[†,‡] Hiroyuki S. Kato,[†] and and Maki Kawai*[,†,‡,§]

RIKEN (The Institute for Chemical and Physical Research), 2-1 Hirosawa, Wako-shi, Saitama 351-0198, Japan, Department of Physics, Gakushuin University, 1-5-1 Mejiro, Toshima-ku, Tokyo 171-8588, Japan, and Graduate School of Frontier Sciences, The University of Tokyo, 5-1-5 Kashiwanoha, Kashiwa-shi, Chiba 277-8561, Japan

Received: September 1, 2005; In Final Form: February 19, 2006

Grafting of unsaturated hydrocarbon moieties ($-CH_2-CH=CH_2$, $-CH=CH_2$, $-CH_2-CH=CH-CH_3$, and $-C\equiv CH$) by a C−Si covalent bond was attempted by the Grignard reaction on hydrogen-terminated Si(111) in tetrahydrofuran solutions. The product adsorbates were monitored by vibrational methods of high-resolution electron energy loss spectroscopy and multiple internal infrared reflection absorption spectroscopy, as well as Auger electron spectroscopy. The temperature and the period of reaction were adjusted so as to preserve the unsaturated carbon−carbon bonds. The $-CH_2-CH=CH_2$ group was introduced by a mild reaction condition, with the reservation of the C=C double bond confirmed. The unsaturated bonds in $-CH_2-CH=CH-CH_3$ and $-C\equiv CH$ were also reserved. Only in the case of $-CH=CH_2$ was the reservation of the C=C double bond not realized. Unsaturated hydrocarbon moieties are applicable for further organic modification to introduce functional groups, and are prospective materials in nanofabrication and biological application on silicon wafer surfaces.

1. Introduction

Monolayers of organic adsorbates bonded on silicon wafer surfaces have prospective properties for applications in nanometer-scale industrial technology.[1,2] The covalent-bond linkage in organic adsorbates can mediate the connection of a variety of molecular groups with the outermost Si atoms. Not only the binding chemically functional groups but also the grafting of biochemical polymers such as proteins and DNA can be realized by formation of covalent bonds.[3−6] The fixation of such biomolecules is one of the key issues in fabricating biochemistry−silicon hybrid devices.[7−11]

Within the diversity of organic species, unsaturated hydrocarbon moieties directly bonded to surface Si atoms are expected to act as the reactive sites for further organic synthesis on silicon surfaces. The C=C double bond and C≡C triple bond can accept addition reactions of various reagents, both ionics and radicals. Successive reactions of conventional organic schemes, such as hydration, hydroboration, cycloaddition of olefins, and addition of halogens and hydrogen halides, can be performed by adjusting the reaction conditions suitable for Si wafer surfaces, which are sensitive to oxidation and contamination.

It is then a very basic task to establish the method to deposit unsaturated hydrocarbons on Si surfaces to gain the freedom of successive modification. Adsorption of saturated hydrocarbons, namely, alkyl groups, has been extensively studied with hydrogen-terminated Si surfaces as the starting material. Linford et al.[12] for the first time reported the radical-initiated adsorption of terminally double-bonded olefins on hydrogen-terminated H:Si(111)−(1×1) in the liquid phase, in which relatively long chains of olefins were tested. This work has been taken up by several groups by photoexcited or thermal deposition of long-chain olefins on hydrogen-terminated Si.[13−22] As C=C bonds are reactive with H−Si bonds, attempts have rarely been made to deposit moieties with more than two C=C double bonds with one double bond reserved. Terminally triple-bonded hydrocarbons have been applied under the existence of $C_2H_5AlCl_2$ to deposit C=C moieties just next to the surface Si atoms on porous silicon substrate. [22]

Another possibility is by the reaction of H:Si(111) with Grignard reagents (C_xH_yMgCl(or Br, I)) or alkyllithium reagents (C_xH_yLi) in organic solvents. It was proposed that the organometallic reagents break into the Si−Si back-bonds and are dissociatively adsorbed.[23,24] The magnesium halide moiety or Li was considered to be detached by treatment in acids, leaving Si-terminating hydrogen. Boukherroub et al.[25] reported that even flat H:Si(111) can react with long-chain alkyl Grignard reagents, forming robust, hydrophobic Si surfaces. Yamada et al. found that the terminating hydrogen atoms on the reacting H:Si(111)−(1×1) sites can be partially replaced with CH_3 groups by contact with CH_3MgBr and CF_3COOH treatment.[26] The adlayer was a mixture of CH_3- and H− occupying the surface Si sites randomly.[4] Recently, Fellah et al.[27] made an electrochemical consideration on the reaction of H:Si(111) with Grignard reagent containing a small amount of alkyl halide.

This sort of hydrocarbon adsorbate mixed with Si-terminating hydrogen atoms is convenient for many reasons. As previously pointed out,[28] the Si(111) surface can be terminated with the (1×1) periodicity only by H, methyl, or a species of similar size because of space-filling within the (1×1) unit cell. To accommodate hydrocarbon species larger than ethyl without steric hindrance, it is a natural idea to create a space with terminating H between the hydrocarbon adsorbates. In the case of highly active moieties, the reaction between adsorbates may

* To whom correspondences should be addressed. E-mail: maki@riken.jp.
† RIKEN.
‡ Gakushuin University.
§ The University of Tokyo.

10.1021/jp054968z CCC: $33.50
Published on Web 03/22/2006

occur, which can be avoided by lowering the adsorbate concentration mixed in the H-terminated adlayer. When the hydrocarbon adsorbates are applied for anchoring macromolecules, such as DNA and proteins at Si substrates, the surface concentration of anchoring species should be controlled to match the space-filling of the macromolecule overlayer. The residual anchoring species that remains reactive after connection of macromolecules is not preferable, as such residual species may cause parasitic reactions.

In some previous works, organic adsorbates were deposited on porous Si substrates, often for specific purposes of application.[22−24] Porous Si is advantageous in detecting adsorbates with high sensitivity by infrared absorption and solid-state NMR,[29] as well as for convenience for chemical treatments. The adsorption sites are not uniform on inhomogeneous Si substrates, involving not only SiH but also SiH_2 and SiH_3. Representation of the bondings near the substrate is complicated, and the assessment of impurity is not simple. The most important C−Si bond was not always detected. To establish the surface chemistry of organic deposition accurately, flat wafer surfaces with simple registry structure are necessary.

In this article we report our attempt to introduce unsaturated hydrocarbon moieties on the hydrogen-terminated Si(111) surface by the Grignard reaction. We treated H:Si(111) in tetrahydrofuran (THF) solutions of allylmagnesium chloride (CH_2═$CH-CH_2MgCl$), vinylmagnesium chloride (CH_2═$CHMgCl$), 2-butenylmagnesium chloride (CH_3-CH═$CH-CH_2MgCl$), and ethynylmagnesium bromide (CH≡CMgBr). The product adsorbates were examined in terms of the bonding structure within the adsorbates and the formation of C−Si bonds by high-resolution electron energy loss spectroscopy (HREELS) and multiple internal infrared reflection absorption spectroscopy (MI-IRAS).

Our precursor Grignard reagents contain unsaturated bonds. Therefore, besides the Grignard reaction of interest to us,

$$CH_2{=}CHC_nH_{2n}MgX + H{:}Si(111) \rightarrow CH_2{=}CHC_nH_{2n}{:}Si(111) \quad (X = \text{halogen}, n = 0, 1, 2, ...) \quad (1)$$

the surface hydrosilylation by the double (triple) bond,[12]

$$CH_2{=}CHC_nH_{2n}MgX + H{:}Si(111) \rightarrow XMgC_nH_{2n}C_2H_4{:}Si(111) \quad (2)$$

might also proceed, excited thermally or by stray light. The attachment to the Si surface can take place both at the Mg end and at the C═C (C≡C) bond of the precursor Grignard reagent. If the attachment takes place at both places, a hydrocarbon moiety bridging two surface Si atoms will be formed, such as

$$CH_2{=}CHC_nH_{2n}MgX + 2H{:}Si(111) \rightarrow Si(111){:}C_2H_4C_nH_{2n}{:}Si(111) \quad (3)$$

We sought the optimum reaction conditions so as to enhance the survival of unsaturated bonds and to minimize the amount of byproducts. From the viewpoint of practical application, the target adsorbates should be stable in the atmosphere at room temperature for a reasonable span of time in the laboratory. We therefore adhered to the process at or above room temperature.

We utilized deuterium-terminated Si(111) (D:Si(111)), originally purposing to resolve occasional overlapping of vibrational peaks. Deuterium labeling was also useful to trace the origin of hydrogen atoms incorporated in the products. The rinsing process with acetic acid after the Grignard reaction was supposed to introduce hydrogen attached to surface Si atoms.[23−26] We attempted to clarify this quenching process using CF_3COOD.

2. Experimental Section

The preparation of H:Si(111) substrates for HREELS, Auger electron spectroscopy (AES), and MI-IRAS measurement is described elsewhere in detail.[26,28,30] In short, n-Si(111) wafer pieces were preoxidized in a hot $H_2SO_4 + H_2O_2$ mixture, followed by etching in a NH_4F solution in H_2O or in a 40% KF solution in D_2O to obtain H:Si(111) and D:Si(111), respectively.[31−33]

Dried H/D:Si(111) was placed in a Pyrex Schlenk tube, connected to a reflux condenser and an Ar cylinder for purging to maintain a dry O_2-free environment. A commercial tetrahydrofuran (THF) solution of 2.0 M allylmagnesium chloride (CH_2═$CH-CH_2MgCl$, Aldrich Chemicals), 1.4 M vinylmagnesium chloride (CH_2═$CHMgCl$, Kanto), 0.5 M ethynylmagnesium bromide (CH≡CMgBr, Aldrich), or a homemade solution of 0.5 M 2-butenylmagnesium chloride (CH_3-CH═$CH-CH_2MgCl$) was then injected. The 2-butenylmagnesium chloride solution was prepared by injecting a THF-diluted 1-chloro-2-butene ($Cl-CH_2-CH$═$CH-CH_3$ trans/cis mixture, Aldrich) into an ice-cooled flask containing Mg ribbon and THF purged with Ar. To terminate the Grignard reaction on H:Si(111), the Si wafer was removed into air and rinsed briefly in THF added with 1%w/w CF_3COOH (Kanto). CF_3COOD (Acros, 1% w/w) in THF was used to study the quenching mechanism of Grignard reagent. Then the surface was rinsed with pure H_2O, dried, and washed in 1,1,2-trichloroethane by an ultrasonic cleaner for 2−5 min.

We paid attention to maintain a good vacuum in the sample introductory system into ultrahigh vacuum (UHV) so as not to contaminate the sample during transferring. As described elsewhere,[4,26,31] the UHV sample-introductory device was carefully evacuated by a liquid-N_2-cooled sorption pump. The samples were put into UHV usually within 1 h after completing the rinsing and drying procedure. The details of vibrational detection by HREELS, determination of absolute coverage by AES, and operation of the MI-IRAS spectrometer are the same as described previously.[31−33]

3. Model Calculation of Vibration Frequencies

To identify the adsorbates observed by MI-IRAS and HREELS, it is desirable to establish reference vibrational frequencies assigned to the normal modes of anticipated adspecies. We assumed the geometric structures of adsorbates derived from the precursor reagents, and calculated the vibrational frequencies by a first-principle theoretical method. Then the theoretical frequencies were compared with experimental frequencies of simple molecules containing the adsorbate structures to establish a practical frequency-to-mode relationship. We can recognize the adsorbates accurately by referring to the frequencies formulated by this task.

We built four upright adstructures fixed with one C−Si bond formulated from the precursor Grignard reagents, designated as "allyl" ($-C(1)H_2-C(2)H$═$C(3)H_2$), "vinyl" ($-C(1)H$═$C(2)H_2$), "2-butenyl" ($-C(1)H_2C(2)H$═$C(3)HC(4)H_3$), and "ethynyl" ($-C(1)$≡$C(2)H$). Also, two bridging adstructures, designated as "ethylene" ($-C(1)H_2C(2)H_2-$) from CH_2═$CHMgCl$ and "propylene" ($-C(1)H_2C(2)H_2C(3)H_2-$) from CH_2═$CHCH_2MgCl$ were assumed. The numbering of atoms in a moiety is given starting from the C atom bonded to surface Si. To adapt the adstructures to the molecular-orbital calculation, the substrate

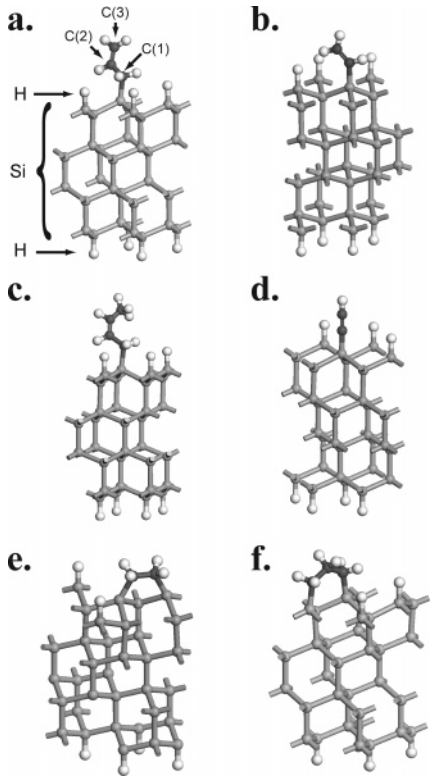

Figure 1. The geometrical cluster structures of adsorbates obtained by DMol[3] DFT optimization. The starting structures for optimization calculation are not far from these structures: (a) allyl moiety, $-C(1)H_2-C(2)H{=}C(3)H_2$, (b) vinyl moiety, $-C(1)H{=}C(2)H_2$, (c) *cis*-2-butenyl moiety, $-C(1)H_2C(2)H{=}C(3)HC(4)H_3$, (d) ethynyl moiety, $-C(1){\equiv}C(2)H$, (e) H_2-ethylene moiety, $-C(1)H_2C(2)H_2-$, and (f) propylene moiety, $-C(1)H_2C(2)H_2C(3)H_2-$. The C atoms in the moieties are numbered starting from the C atom bonded to Si. The underlying substrate cluster is composed of four Si(111)−(2×2) bilayers (32 Si atoms). The 8 dangling bonds on the top and bottom of this cluster are all terminated with H atoms, and one of the hydrogen atoms on the top is replaced with the target moiety.

Si crystal was modeled as a Si cluster composed of four Si-(111)−(2×2) bilayers (thickness = 1.52 nm). To make these models closer to reality, just one hydrocarbon moiety is placed on the top side, and the surrounding Si sites and the bottom surface are all hydrogen terminated. This full-surface termination policy also makes the calculation simple by putting dangling bonds out of concern. The bonding structures of 6 model clusters are shown in Figure 1.

Then we performed a density-function-theory (DFT) geometric energy optimization by the aid of a commercial program package (Accelrys DMol[3] version 3.0[34−36]) installed on RIKEN's Super Combined Cluster System (RSCC) with 2048 parallel LINUX central processing units. The structures in Figure 1, added with a 1.5-nm-tick vacuum slab, were used as the starting structures of geometrical optimization under the 3-dimensional periodic boundary condition. For the energy calculation, the double-numeric quality basis set with polarization functions (DNP), the semicore pseudopotentials of atoms, and the generalized gradient corrected (GGA) functional by revised Perdew−Burke−Ernzerhof (RPBE)[37,38] were employed. A Fermi smearing of 1.36 eV and a real-space cutoff of 0.35 nm were used to improve computational utility. The tolerances of energy, gradient, and displacement convergence were 0.003 eV, 3 eV/nm, and 0.005 nm, respectively. The Hessian matrix was finally calculated and the characteristic vibration modes were obtained. No empirical corrections, such as multiplication of scaling factors, were applied to the numbers. The obtained frequencies are genuinely first-principle results.

Table 1 shows the frequencies selected from the results of calculation, which represent the key modes useful in recognizing the internal bonds of adsorbates. The stretching modes of C−H, C=C and C−Si, CH_3 umbrella, $=CH_2$ scissors, and $=CH_2$ out-of-plane bending are important in confirming the existence of our target adsorbates. The CH_2 twisting, rocking, wagging, and asymmetric bending modes are located in the narrow range from 900 to 1300 cm^{-1} and are difficult to distinguish from each other in real spectra. Table 1 also carries the frequencies of infrared or Raman spectra measured for the gas phase or the liquid phase of simple molecules similar to the adsorbates.[39,40] It is seen that the calculated frequencies match fairly well with the real frequencies assigned to the normal modes by the well-established group frequency method.[41,42]

A notable result of calculation is that the C−Si stretching frequency significantly depends on the size of the fixed moiety. It varies from 589 (ethynyl) to 499 cm^{-1} (2-butenyl) for the single-site adsorbates. The C−Si vibrator is naturally approximated consisting of the infinitive mass of substrate and a rigid mass of hydrocarbon connected with a unique C−Si force constant. Then the frequency is supposed to be an apparently decreasing function of the mass of the hydrocarbon moiety. This tendency was already discovered in some experimental results.[28,43,44] These calculated frequencies might not be accurate but are useful in recognizing this tendency of frequency variation in the determination of each of the bonding structures of adsorbates.

This calculation also provides the optimized total electronic energy of each model structure, and it is interesting to predict the stability of adsorbates by comparing these energies. In Figure 1 structures "a" (allyl) and "f" (propylene) are isomers of each other, and the total energy difference allyl − propylene is +5.6 kcal mol^{-1}, indicating that the double-bonded allyl isomer is less stable than the double-anchored propylene isomer. Radical $^{\bullet}CH_2-CH_2-CH_2$:Si + $^{\bullet}$Si species, a possible intermediate of interconversion between "a" and "f", was calculated to have a total energy higher by 2 kcal mol^{-1} than "a". The total energy difference "b" (vinyl) − "e" (ethylene) is +7.0 kcal mol^{-1}. If the conversion reaction from "b" to "e" takes place, it probably involves $^{\bullet}CH_2-CH_2$:Si + $^{\bullet}$Si radical species as an intermediate, of which the calculated total energy is larger by just 0.4 kcal mol^{-1} than structure "b". The activation energy of reaction "b" → "c" is then considered to be small, and this conversion might proceed easily.

4. Results and Discussion

4.1. Adsorption of the Allyl Group, $-CH_2-CH{=}CH_2$. It was important in this study to adjust the temperature and period of the Grignard reaction to obtain the desired adsorbates with adequately large uptake at the surface. The condition was optimized by monitoring the C−H stretching region of MI-IRAS after a fixed reaction procedure with varying the solution temperature and the time from reagent pouring to specimen removal out of the solution.

Figure 2 shows the traces of MI-IRAS during the survey for H:Si(111) in 2 M $CH_2{=}CHCH_2MgCl$ in THF, with the solution temperature varied from 35 to 55 °C. The spectra obtained at 35 °C of the solution temperature involve a broad band centered at 2920 cm^{-1}, and two weak peaks above 3055 and 3150 cm^{-1}. Referring to the frequencies shown in Table 1 for allyl adsorbate and propylene adsorbate, we can judge the modes below 3000 cm^{-1} to be the stretching modes of H attached to the sp^3-carbon,

TABLE 1: The Key Vibrational Frequencies (cm^{-1}) Calculated for the Nominated Normal Modes for Allyl, Vinyl, 2-Butenyl, Ethynyl, Ethylene, and Propylene Adsorbates Placed in H:Si(111)−(1×1) As Illustrated in Figure 1[a]

a. Allyl Adsorbate Si−C(1)H_2−C(2)═C(3)H_2

simulated freq	normal mode	IR freq of CH_2═$CHCH_2F$ gas[40]	simulated freq	normal mode	IR freq of CH_2═$CHCH_2F$ gas[40]
3126	C(3)H_2═ asym str/═C(2)H str	3104	1430	C(2)═C(3) str	1652
2993	C(3)H_2− sym str/═C(2)H str	2959	1377	C(3)H_2═ scissors motion	1426
2943	C(1)H_2− asym str	2940	1232	C(2)H═ in-plane bending	1376
2915	C(1)H_2− asym str	2902	911	C(3)H_2═ out-of-plane bending (wagging)	1014
2848	C(1)H_2 sym str	2883			
1986	H−Si str		646	Si−H bending	
			564	C(1)−Si str	

b. Vinyl Adsorbate Si−C(1)H═C(2)H_2

simulated freq	normal mode	IR freq of CH_2═CHF gas[40]	simulated freq (cm^{-1})	normal mode	IR freq of CH_2═CHF gas[40]
3119	C(2)H_2═ asym str	3156	982	C(2)H_2═ in-plane bending (rocking)	1130
2991	C(1)H str	3117			
2975	C(2)H_2 sym str	3076	908	C(2)H_2/C(1)H inphase out-of-plane bending	929
1916	H−Si str				
1425	C(1)═C(2) str/C(2)H_2═ antiphase scissors motion	1671	847	C(2)H_2/C(1)H antiphase out-of-plane bending	862
1276	C(1)═C(2) str/C(2)H_2═ inphase scissors motion	1634	620	H−Si bending	
			569	C(1)−Si str	
1204	C(1)H inplane bending	1170			

c. 2-Butenyl Adsorbate Si−C(1)H_2−C(2)H═C(3)H−C(4)H_3

simulated freq	normal mode	IR freq of *trans/cis*-CH_3CH═$CHCH_2Cl$ liquid (this work)	simulated freq	normal mode	IR freq of *trans/cis*-CH_3CH═$CHCH_2Cl$ liquid (this work)
3069	HC(2)═C(3)H sym str	3096	1311	C(1)H_2 scissors motion	1311
3016	HC(2)═C(3)H asym str	3036	1141	C(2)H═C(3)H inplane sym bending	1174
2924	C(4)H_3 asym str	2955			
2921	C(1)H_2 asym str	2940	1063	C(3)−C(4) str	1069
2846	C(4)H_3 sym str	2887	738	C(2)H═C(3)H asym out-of-plane bending	951
2838	C(1)H_2 sym str	2860			
2040	H−Si str		668	H−Si bending	
1480	C(2)═C(3) str	1669	522	C(2)H═C(3)H sym out-of-plane bending	871
1360	C(2)H═C(3)H inplane asym bending	1254			
1338	C(4)H_3 umbrella motion	1378	477	C(1)−Si str	

d. Ethynyl Adsorbate Si−C(1)≡C(2)H

simulated freq	normal mode	IR and Raman freq of HC≡CH gas[39]	simulated freq	normal mode	IR and Raman freq of HC≡CH gas[39]
3320	C(2)−H str	3374, 3289	658	H−Si bending	
			589	C(1)−Si str	
1948	H−Si str		585	C(1)−Si str	
1790	C(1)≡C(2) str, inphase with H−Si str	1974	499	H−C(2)≡C(1) bending	730
1694	C(1)≡C(2) str, antiphase with H−Si str		493	H−C(2)≡C(1) bending	612

e. Ethylene Adsorbate Si−C(1)H_2−C(2)H_2−Si

simulated freq	normal mode	IR freq of $BrCH_2CH_2Br$ gas[40]	simulated freq	normal mode	IR freq of $BrCH_2CH_2Br$ gas[40]
2964	C(1)H_2/C(2)H_2 antiphase asym str	2994	1323	C(1)H_2/C(2)H_2 inphase scissors motion	1427
2956	C(1)H_2/C(2)H_2 inphase asym str	2974			
2856	C(1)H_2/C(2)H_2 antiphase sym str	2886	852	C(1)−C(2) str	841
2844	C(1)H_2/C(2)H_2 inphase sym str	2878	636	H−Si bending	
1983	H−Si str		499	Si−C(1)−C(2)−Si asym str	
1342	C(1)H_2/C(2)H_2 antiphase scissors motion	1450			

f. Propylene Adsorbate Si−C(1)H_2−C(2)H_2−C(3)H_2−Si

simulated freq	normal mode	IR freq of $BrCH_2$-CH_2CH_2Br gas[40]	simulated freq	normal mode	IR freq of $BrCH_2$-CH_2CH_2Br gas[40]
2923	C(1)H_2/C(3)H_2 antiphase asym str	3023	1358	C(1)H_2/C(3)H_2 antiphase scissors motion	1352
2922	C(1)H_2/C(3)H_2 inphase asym str	2978			
2870	C(1)H_2/C(3)H_2 inphase sym str	2932	1328	C(2)H_2 scissors motion	1356
2852	C(1)H_2/C(3)H_2 antiphase sym str	2921	667	H−Si bending	
2801	C(2)H_2 asym str	2870	532	C(1)−Si/C(3)−Si asym str	
2764	C(2)H_2 sym str	2830	530	C(2)−C(1)−Si/C(2)−C(3)−Si sym bending	
2092	H−Si str				
1371	C(1)H_2/C(3)H_2 sym scissors motion	1441			

[a] The frequencies were obtained by density-function-theory based molecular-orbital calculation package Accelrys "Dmol[3]" version 3.0 (refs 34−36). The experimental frequencies found in the literature or by our own experiment are also listed, associated with the normal modes.

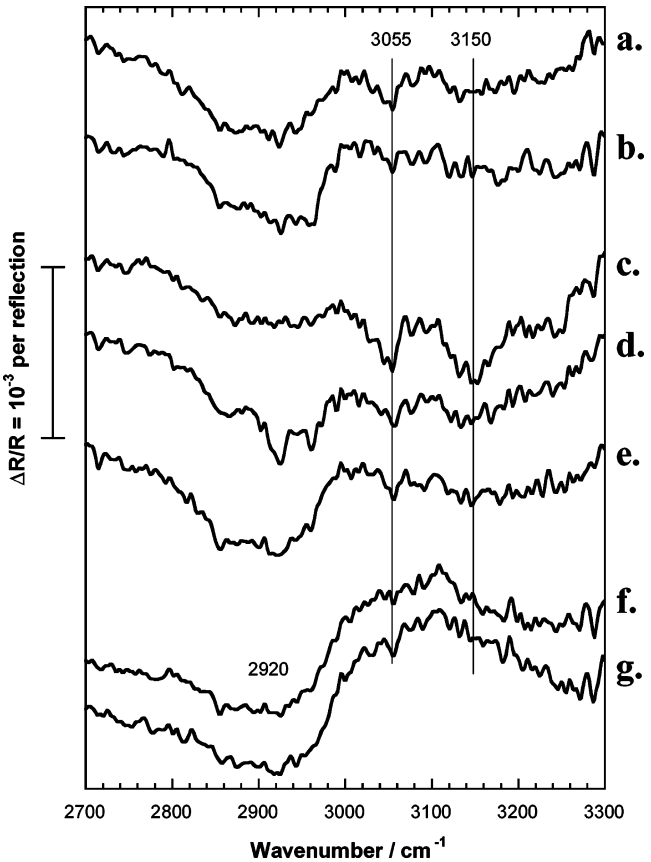

Figure 2. MI-IRAS of H:Si(111) treated in 2.0 M CH_2═$CHCH_2MgCl$/THF, and rinsed in 1% w/w CF_3COOH/THF, H_2O, and $CHCl_2CH_2Cl$. Resolution setting = 4.0 cm^{-1}, 15 000 scans accumulated for each spectrum: (a) reaction solution temperature = 35 °C, reaction time = 10 min; (b) reaction solution temperature = 35 °C, reaction time = 20 min; (c) reaction solution temperature = 45 °C, reaction time = 5 min (the AES atomic C/Si ratio was 0.28); (d) reaction solution temperature = 45 °C, reaction time = 10 min; (e) reaction solution temperature = 45 °C, reaction time = 15 min; (f) reaction solution temperature = 55 °C, reaction time = 5 min; and (g) reaction solution temperature = 55 °C, reaction time = 10 min. The vibration frequency is presented as wavenumber in units of cm^{-1}.

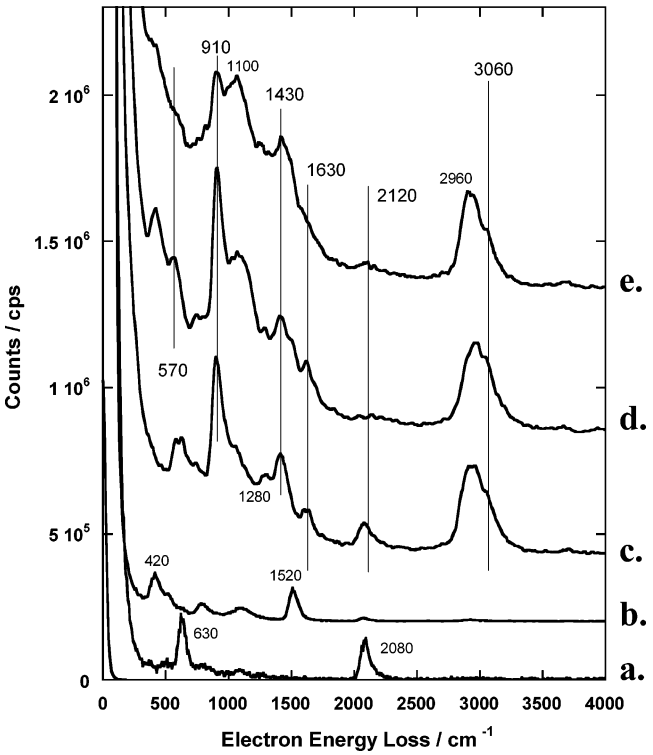

Figure 3. HREELS of H:Si(111) and D:Si(111) treated in 2.0 M CH_2═$CHCH_2MgCl$/THF at 35 °C solution temperature for 5 min. HREELS was recorded by an incident electron energy of 2.84 eV with the angles of incidence and exit fixed at 60° from the surface normal. (a) H:Si(111) prepared by etching O/Si(111) in 40% w/w NH_4F + 1% w/w $(NH_4)_2SO_3/H_2O$ for 10 min. The count axis is magnified by, ×500. (b) D:Si(111) prepared by etching O/Si(111) in 40% w/w KF + 1% w/w K_2SO_3/D_2O (>99.5% isotope enrichment) for 210 min, ×200. (c) H:Si(111) after the Grignard reaction and rinsing in 1% CF_3COOD/THF, H_2O, and $CHCl_2CH_2Cl$, ×2000. AES atomic C/Si ratio = 0.28. (d) D:Si(111) after the Grignard reaction and rinsing in 1% CF_3COOD/THF, H_2O, and $CHCl_2CH_2Cl$, ×2000. The AES atomic C/Si ratio was 0.28. (e) D:Si(111) after the Grignard reaction and rinsing in 1% CF_3-$COOH$/THF, H_2O, and $CHCl_2CH_2Cl$, ×3333. The vibration frequency is presented as electron-energy loss, with the units converted from meV to cm^{-1} (8.06 cm^{-1} = 1 meV). The elastic peak is indicated at the bottom, ×1.

and the modes above 3000 cm^{-1} to be those attached to the sp^2-carbon. The emergence of peaks above 3000 cm^{-1} indicates what the C═C bonds contained. On curves a and b in Figure 2, the peaks at 3055 and 3150 cm^{-1} are not so strong, and the broad band at 2920 cm^{-1} is significant. The surfaces of curves a and b might contain C═C double bonds, but the major part was saturated hydrocarbons.

On curve c recorded after reaction at 45 °C for 5 min, the peaks at 3055 and 3150 cm^{-1} are prominent and the broad peak at 2920 cm^{-1} is depleted. The adsorbates containing C═C bonds became major on the surface. The AES atomic C/Si ratio measured on the same surface was 0.28, converted to 9% of Si(111) termination by pure allyl (C_3) groups. Mg, Cl, O, or other contaminating elements were below the noise level of AES. The purity of this adlayer as an allyl monolayer will be discussed later by viewing HREEL spectra. As the reaction time was elongated (curves d and e), the sp^2 peaks were depleted and the broad peak for saturated hydrocarbons was enhanced. AES indicated a continuous increase of carbon uptake according to the reaction time. The C═C double bonds were altered by reactions with the H-terminated surface or other neighboring adsorbates when the coverage exceeded a certain level. After the Grignard reaction at 55 °C, the sp^3 peak at 2920 cm^{-1} was always strong, and the peaks at 3055 and 3150 cm^{-1} were negligibly small. The completion of reaction in CH_2═$CHCH_2$-$MgCl$/THF was apparently more rapid than that in the cases of Grignard reagents of saturated linear alkyls, which usually takes longer than 4 h.[3,4]

The condition to obtain the highest content of unsaturated adsorbates from CH_2═$CHCH_2MgCl$/THF was optimized as above, and HREELS was employed to examine the chemical bonds on surfaces prepared with this condition. Figure 3 shows HREELS for H:Si(111) and D:Si(111) before and after treatment in 2 M CH_2═$CHCH_2MgCl$/THF at 45 °C for 5 min, rinsed in an 1% w/w THF solution of CF_3COOH or CF_3COOD, to study the effect of quenching at the same time.

Curves c and d are informative in recognizing the covalent bonds and the process of deposition. On curve c, the modes characteristic to the C═C double bond are found at 3060, 1630, 1430, and 910 cm^{-1}, which are not seen as a set in the spectra of CH_3:Si(111), a typical saturated hydrocarbon monolayer.[26,28] The shoulder at 3060 cm^{-1} corresponds to the composite of MI-IRAS peaks at 3055 and 3150 cm^{-1}. The major peak at 2960 cm^{-1} is considered to be composed of C(3)H_2═ symmetric stretching coupled with stretching motions of ═C(2)H or C(1)-H_2 by referring to the calculated frequencies in Table 1. There might be a contribution to this peak from entirely saturated

hydrocarbon moieties, which can be estimated from other parts of the spectra.

The prominent peak at 1630 cm^{-1} indicates the existence of C═C double bonds within the adspecies. This C═C stretching frequency is nearly exactly equal to that in the allyl fluoride molecule.[40] The peak at 1430 cm^{-1} is assigned to the CH_2═ scissors motion that is characteristic to sp^2-carbon terminated by two hydrogen atoms. The sharp intense peak at 910 cm^{-1} is assigned to the bending motion of H on C═C sp^2 carbons, vertical to the sp^2 valence plane. This frequency exactly matches the result of calculation and the peak position of gaseous IR spectra in Table 1. This "out-of-plane" bending vibration is frequently observed as an intense peak in HREELS of unsaturated hydrocarbons.[45] These key peaks at 3060, 1630, 1430, and 910 cm^{-1} provide strong evidence for inclusion of $-CH═CH_2$ groups as the major part of the adlayer.

The peaks at 2080 and 630 cm^{-1} are assigned to H−Si stretching and bending motions, respectively, of the terminating hydrogen atoms left over from the Grignard reaction. As mentioned above, AES indicated 9% coverage by the allyl group, and 91% of the surface Si atoms were considered to be terminated still with H. Although curve c was recorded after CF_3COOD rinse, the D−Si signals expected at 1520 and 420 cm^{-1} (see curve b) are not visibly involved. This fact indicates that the quenching of MgCl groups by CF_3COOD after Si−Si back-bond breakage to form D−Si bonds is not a major route of deposition. According to the Å-scale images of H:Si(111) treated in Grignard reagents by scanning tunneling microscopy (STM),[3,4] we could not observe the massive breakage of Si−Si back-bonds resulting in formation of pits.[25] The Grignard-modified surfaces were usually as flat as the starting H:Si(111). The replacement of Si-terminating H with MgCl groups on the surface in contact with the Grignard reagent solution is not probable, either. The deposition of hydrocarbon groups on H:Si(111) by the Grignard reaction should then be formulated as a single-site reaction. This is also supported by the absence of H−Si signal on D:Si(111) treated in CH_3MgBr/THF and rinsed in CF_3COOH.[26] In this sense, the quenching procedure by acid does not contribute to the main process. It is, however, convenient to use CF_3COOH/THF to remove the residual Grignard reagent from the wafer surface quickly and thoroughly.

Fellah et al.[27] proposed an interesting mechanism of the Grignard reaction on H:Si(111) involving a trace amount of alkyl halides in the Grignard reagent mediating the overall reaction. We also studied photoadsorption of alkyl halide on H:Si(111), which produces an alkyl adlayer without halogen deposition.[46] Although the formulation of a single-site reaction mechanism is complicated,[27] a consistent explanation for the ejection of terminating H is induced by the existence of alkyl halide as a co-reactant.

On curves c in Figure 3, the shoulder at 1100 cm^{-1} is assigned to residual SiO_2 impurity inherited from the starting H:Si(111) surface. The group frequencies of rocking or twisting motions of CH_2 might be placed in this range according to the DFT calculation; however, no intense peak is located in the IR spectra of allyl compounds.[40] The amount of SiO_2 to yield this intensity of signal is estimated to be below 0.3% of monolayer by the method described elsewhere.[26] In addition, in the frequency range from 700 to 1600 cm^{-1}, the baseline of peaks is slightly elevated, forming a sort of continuum. This elevation corresponds to the C−H bending motions of a small amount of saturated hydrocarbons staying on the surface.

Figure 3d shows the spectrum on D:Si(111) treated in $CH_2═CHCH_2MgCl$/THF and rinsed in CF_3COOD/THF. The set of peaks attributed to the $-CH═CH_2$ group is identical with that on curve c. The stretching and bending motions were relocated to 1520 and 420 cm^{-1} for D−Si. The small shoulder at 1520 cm^{-1} represents the existence of residual D. By this relocation, the overlapping of peaks in the range near 600 cm^{-1} was resolved. The H−Si bending peak at 630 cm^{-1} was relocated to 420 cm^{-1} as D−Si bending, and an eminent peak was revealed at 570 cm^{-1}. The satellite phonon peaks at 510 and 800 cm^{-1} associated with the H−Si bending peak are relocated to 300 and 510 cm^{-1}, respectively, with D−Si.[30] The peak at 570 cm^{-1} on curve d is obviously different from this right-side satellite at 510 cm^{-1} in position and in relative height. According to the result of calculation in Table 1, this peak is nearest to the frequency of C−Si stretching (=565 cm^{-1}). We have revealed the C−Si bond, the most important bond in organic adsorbates on Si, formed in the unsaturated hydrocarbon Grignard reagent.

Another feature on curve d is a weak, broad peak centered at 2120 cm^{-1}, which is slightly higher than 2080 cm^{-1} of the H−Si stretching peak introduced to D:Si(111) as an impurity, as recognized on the starting surface. This peak may be due to new C−D bonds within the adsorbates or Si−H bonds formed in the vicinity of the adsorbates. These bonds are produced by incorporation of surface-terminating D into the adsorbate, or a certain sort of H/D isotope exchange reaction between the surface and adsorbate. This 2120 cm^{-1} peak is weaker than the C−H stretching peak at 2960 cm^{-1} by more than an order of magnitude, and such side reactions were minor under the present deposition condition. The SiO_2 peak at 1100 cm^{-1} is stronger than that on curve c, because of the difficulty in removing oxide SiO_2 thoroughly in KF/D_2O solution.[30]

Figure 3e shows the same $CH_2═CHCH_2MgCl$-treated /D:Si(111) surface rinsed in CF_3COOH/THF. The starting D:Si(111) surface contained more SiO_2 than the other surfaces, and the spectral signal was weakened with smearing of featuring peaks. It is again seen that the inclusion of H from the quenching CF_3COOH could not be the major reaction route as no evident enhancement of the H−Si signals was detected.

Judging from these spectroscopic findings, we can conclude that the reactant allyl groups were mostly reserved as allyl moieties fixed by C−Si covalent bonds on Si(111) surrounded by H-terminated Si sites. The uptake of allyl groups (~9%) is large enough to conduct succeeding reactions to modify the C═C part and to detect the products by vibration spectroscopy.

4.2. Adsorption of the Vinyl Group, $-CH═CH_2$. The adsorption process of the vinyl group delivered from Grignard reagent was surveyed by monitoring by MI-IRAS and AES. The $CH_2═CHMgCl$/THF solution was apparently more reactive than linear alkyl Grignard reagents. The uptake of adsorbates reached a saturation level (approximately 15% of a monolayer) within a few minutes at room temperature. Figure 4 shows MI-IRAS of H:Si(111) treated in 1.4 M $CH_2═CHMgCl$/THF for some solution temperatures and reaction times. The spectrum obtained after the reaction for 3 min at 20 °C of the solution temperature (Figure 4a) involves a pair of sharp peaks at 2930 and 2850 cm^{-1}. The positions and intensity ratio of these peaks are similar to those of long-chain alkyl ($CH_3(CH_2)_n-$) adsorbates,[3,4,30] indicating that the adsorbates are composed mainly of CH_2 groups. The signals above 3000 cm^{-1} associated with stretching motions of hydrogen on sp^2 C═C carbons were not detected.

As the reaction time was elongated, these CH_2 peaks were broadened and merged into a spread feature (Figure 4b). This is due to the emergence of CH_2 groups in various bonding

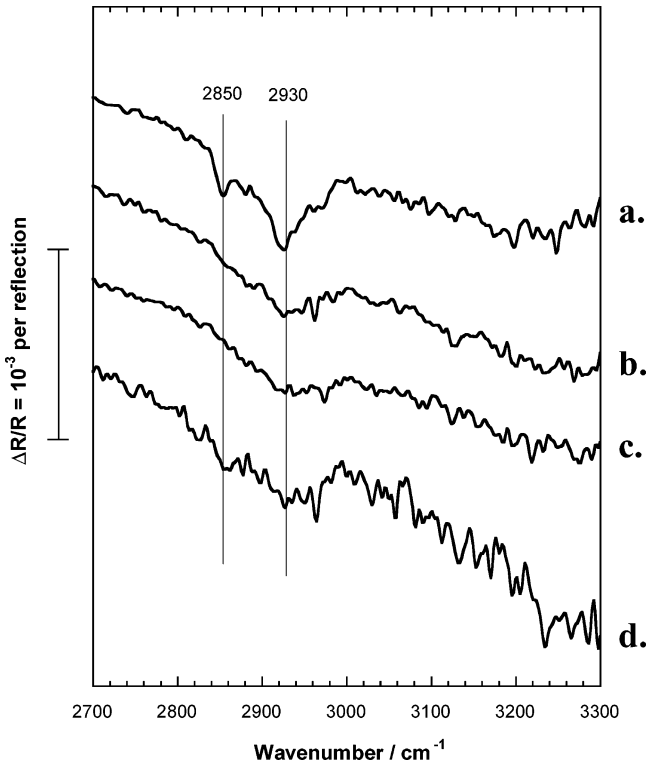

Figure 4. MI-IRAS of H:Si(111) treated in 1.4 M CH_2═CHMgCl/THF and rinsed in 1% w/w CF_3COOH/THF, H_2O, and $CHCl_2CH_2Cl$. Resolution setting = 4.0 cm^{-1}, 15 000 scans accumulated for each spectrum: (a) reaction solution temperature = 20 °C, reaction time = 3 min (AES atomic C/Si ratio = 0.28); (b) reaction solution temperature = 20 °C, reaction time = 5 min; (c) reaction solution temperature = 65 °C, reaction time = 5 min; and (d) reaction solution temperature = 65 °C, reaction time = 120 min.

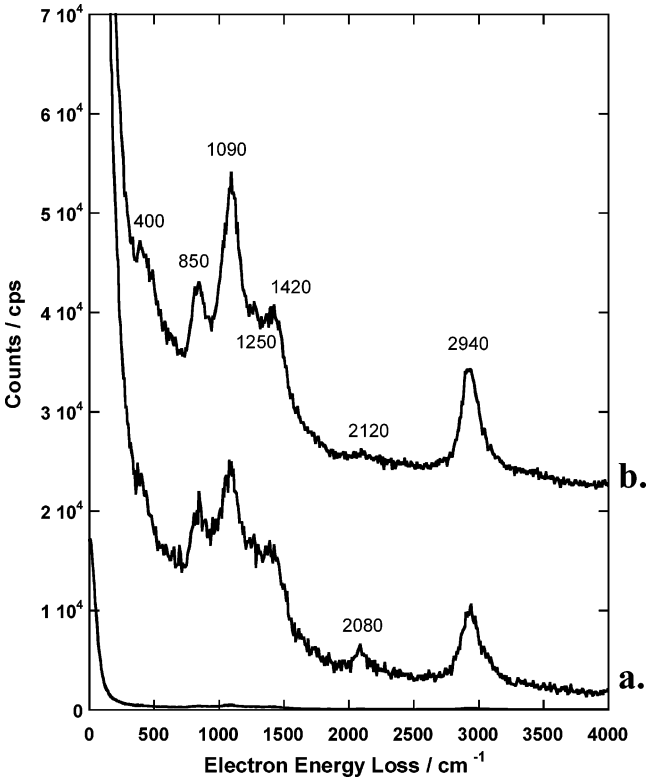

Figure 5. HREELS of H:Si(111) and D:Si(111) treated in 1.4 M CH_2═CHMgCl/THF at 20 °C solution temperature for 3 min: (a) H:Si(111) after the Grignard reaction and rinsing in 1% CF_3COOH/THF, H_2O, and $CHCl_2CH_2Cl$, ×50 (AES atomic C/Si ratio = 0.28); and (b) D:Si-(111) after the Grignard reaction and rinsing in 1% CF_3COOD/THF, H_2O, and $CHCl_2CH_2Cl$, ×50.

configurations. The adlayer was inhomogeneous in this sense. At 65 °C solution temperature, the signal in the region from 2800 to 3000 cm^{-1} was always a spread feature, with no peaks above 3000 cm^{-1} (Figure 4c,d). The adlayer prepared at 20 °C and 3 min was the only choice for us as a well-ordered surface.

Figure 5 shows HREELS of H:Si(111) and D:Si(111) treated in 1.4 M CH_2═CHMgCl/THF at 20 °C and 3 min. It is notable that the intensity of the elastic peak was broadened and weakened in intensity compared to that of H/D:Si(111) within this short period of reaction. The H/D−Si bending signals (630 cm^{-1}/420 cm^{-1}) are invisible compared to the spectra for the allyl group, although the AES atomic C/Si ratio was similar. These facts can be interpreted due to mixed adspecies. The loss peaks are broad, indicating that many kinds of bonds existed on the surfaces. The peak at 2940 cm^{-1} is assigned to the C−H stretching motions in saturated hydrocarbons. No apparent peaks are seen above 3000 cm^{-1}. The C═C stretching signal, expected near 1600 cm^{-1}, is also missing. The peaks at 1420 and 1250 cm^{-1} are related to C−H bending modes. The signal at 1090 cm^{-1} involves a contribution from the SiO_2 impurity. The peak detected at 850 cm^{-1} corresponds to the C−C stretching calculated for ethylene adsorbate (=851 cm^{-1}) and one separate peak at 840 cm^{-1} in the IR spectrum of 1,2-dibromoethane.[40] The spectrum of CH_2═CHF involves no signal here.[40] The vibration mode seen at 400 cm^{-1} in Figure 5a,b is associated with the C−Si stretching by referring to the results of calculation for vinyl and ethylene. The calculated C−Si frequency of ethylene adsorbate (=499 cm^{-1}) is closer to this.

By MI-IRAS and HREELS, we could not recognize any evidence for the reservation of C═C double bonds delivered in CH_2═CHMgCl at or above room temperature. The absence of the C═C double bond can be explained by the two-site reaction, which is schematized as a special case of eq 3 on the D:Si-(111) surface. The surface D is incorporated into the adsorbate, and actually Figure 5b recorded on D:Si(111) contains a weak signal at 2120 cm^{-1} assigned to C−D stretching. If $-CH_2-$CHD− covers the surface, then the C−H/C−D signal intensity ratio should be comparable to 3:1. In Figure 5b the content of C−D is obviously smaller than this level. Probably more complicated adsorbates mainly composed of CH_2 groups were formed. Another mechanism, such as C═C consumption in the reaction between adsorbates, should be considered. For example, two neighboring vinyl adsorbates might undergo cycloaddition right after deposition by the Grignard reaction.

4.3. Adsorption of the 2-Butenyl Group, $-CH_2-CH=CH-CH_3$. The C═C double bond in $-C(1)H_2-C(2)H=C(3)H-C(4)H_3$ is isolated from the anchoring Si atom and the other end of the moiety. The 2-butenyl adsorbate is anticipated to possess a better stability than vinyl. The uptake of adsorbates in 2-butenylmagnesium chloride/THF increased slowly. We recognized the saturation of uptake in 16 h at 60 °C solution temperature by AES. This low reaction rate is comparable to those of saturated linear-chain alkyl groups.

Figure 6b shows HREELS of H:Si(111) treated in 0.5 M CH_3-CH═$CHCH_2MgCl$/THF at 60 °C solution temperature for 16 h. The AES atomic C/Si ratio was 0.77, equivalent to 0.19 monolayers of 2-butenyl. Discrete peaks are seen at 2940, 1660, 1460, and 1050 cm^{-1}. The C−H stretching peak at 2940 cm^{-1} is slightly asymmetric with a slight broadening toward high frequency. This is a sign of $-CH=CH-$ sp^2 hydrogen atoms contributing to the major $-CH_3$ and $-CH_2-$ signals centered at 2960 cm^{-1}. The peak at 1660 cm^{-1}, assigned to C═C stretching, matches well the calculated frequency and the IR

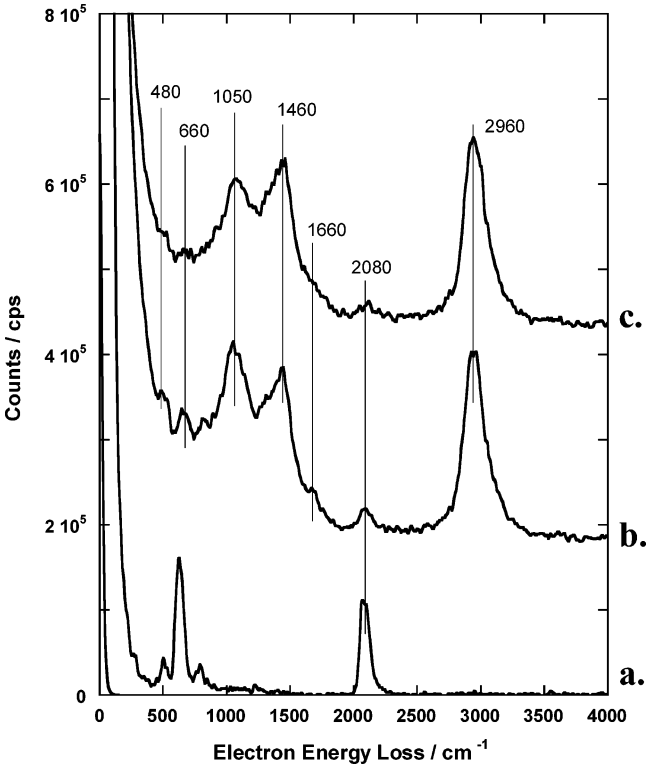

Figure 6. HREELS of H:Si(111) treated in 0.5 M $CH_3CH{=}CHCH_2$-MgCl/THF at 60 °C solution temperature for 16 h: (a) H:Si(111) before reaction, ×1000; (b) H:Si(111) after the Grignard reaction and rinsing in 1% CF_3COOH/THF, H_2O, and $CHCl_2CH_2Cl$, ×500 (AES atomic C/Si ratio = 0.77, incident electron energy = 2.84 eV, incident angle = 60°, exit angle = 60°; (c) the same surface as b (exit angle = 65°, ×500).

peak position in 1-chloro-2-butene listed in Table 1. It is notable that the C=C double bonds were reserved at a relatively high solution temperature. Many vibration modes are predicted in the region below 1500 cm^{-1}, and the broad peak at 1460 cm^{-1} is supposed to be composed of various C−H bending modes. The peak at 1050 cm^{-1} is associated with C(1)−C(2) and C(3)−C(4) single-bond stretching motions. It probably also includes the impurity SiO_2 signal. The peaks at 2080 and 660 cm^{-1} originated from the residual H−Si bonds. The peak at 480 cm^{-1} is assigned to the C−Si stretching motion derived by the calculation.

The origins of loss peaks can be understood better by viewing the off-specular spectrum (Figure 6c). In comparing curves b and c of Figure 6, it is seen that the H−Si originating peaks are significantly weakened in the off-specular spectrum. The adsorbate-originating peaks, one at 480 cm^{-1} in particular, are better isolated. The depleted portion of the peak at 1050 cm^{-1} is mainly of the contaminant SiO_2, as the intensity of the SiO_2 loss peak changes sensitively to the detection angle.[26] The peak of C=C stretching at 1660 cm^{-1} is also significantly weakened. The process of electron energy loss by C−H bonds is usually explained by impact scattering, characterized by a broad angular distribution of loss electrons.[47] In contrast, the major part of excitation of the C=C stretching in this case seems to be in the category of dipole scattering.[47]

As observed, 2-butenyl groups delivered in the Grignard reagent build up a coverage near 20% of a monolayer, with the C=C double bonds reserved. The parasitic reactions that diminish C=C bonds in the solution at 60 °C seem to be minor.

4.4. Adsorption of the Ethynyl Group, −C≡CH. Adsorption of ethynyl groups was performed by treating H:Si(111)/D:Si(111) in 0.5 M CH≡CMgBr/THF. The Si surfaces were frequently contaminated with SiO_2 in the treatment in this solution in the temperature range below 60 °C. This solution tended to form gray precipitate upon heating. We attempted to optimize the solution temperature and reaction time, aiming for the minimum SiO_2 coverage.

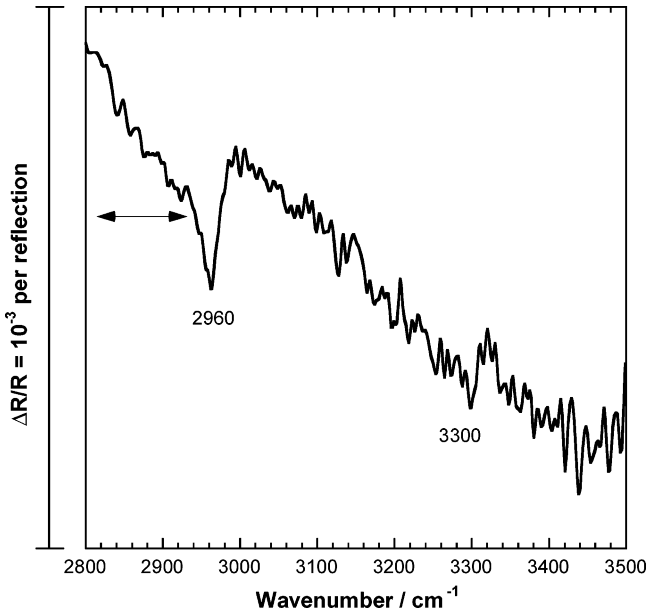

Figure 7. MI-IRAS of H:Si(111) treated in 0.5 M CH≡CMgBr/THF, and rinsed in 1% w/w CF_3COOH/THF, H_2O, and $CHCl_2CH_2Cl$. Resolution setting = 4.0 cm^{-1}, 15 000 scans accumulated for each spectrum. The SiO_2 filter was not used. Reaction solution temperature = 65 °C, reaction time = 255 min. AES atomic C/Si ratio = 0.55. The arrowed region corresponds to the $-CH_2-$ stretching modes.

The MI-IRAS in Figure 7 was obtained after the Grignard reaction at 60 °C for 300 min followed by rinsing in CF_3COOH/THF. This spectrum contains a weak signal centered at 3300 cm^{-1}, attributed to C−H stretching in the −C≡CH moiety. A more intense peak is seen at 2960 cm^{-1}, accompanied by a low-frequency tail down to 2840 cm^{-1}. The peak at 2960 cm^{-1} represents the asymmetric stretching motion of the CH_3 group, and the tailing part is assigned to the stretching motions of CH_2 groups in various environments. The H:Si(111) surface treated in the CH≡CMgBr/THF solution was grafted with −C≡C−H groups and saturated hydrocarbon moieties. By referring to the infrared spectra on alkyl groups on Si,[4,30] it can be estimated from the intensities of the 2960 cm^{-1} signal and the tailing part that this saturated hydrocarbon impurity is composed of alkyl groups from methyl to butyl.

Figure 8 shows HREELS of H:Si(111) and D:Si(111) treated in 0.5 M CH≡CMgBr/THF solution at 60 °C for 300 min followed by rinsing in 1% CF_3COOH/THF. The spectra on both H:Si(111) and D:Si(111) contain the C−H stretching signals at 3310 cm^{-1} assigned to −C≡CH groups and at 2960 cm^{-1} assigned to saturated hydrocarbons. The peak intensity ratio of 3310 cm^{-1}:2960 cm^{-1} was uncontrollable but usually near 1:1. The AES C/Si ratio was 0.55, which includes the amount of saturated hydrocarbons.

On D:Si(111), the hydrogen-termination signals are relocated as D−Si signals at 1520 and 420 cm^{-1}, and the adsorbate signals overlapped by the signals near 2080 and 680 cm^{-1} on H:Si-(111) were resolved. The signal at 2020 cm^{-1} on curve b is considered to originate purely from the C≡C stretching motion, since the residual H−Si stretching signal as the impurity for the D−Si species should be negligibly small in proportion to

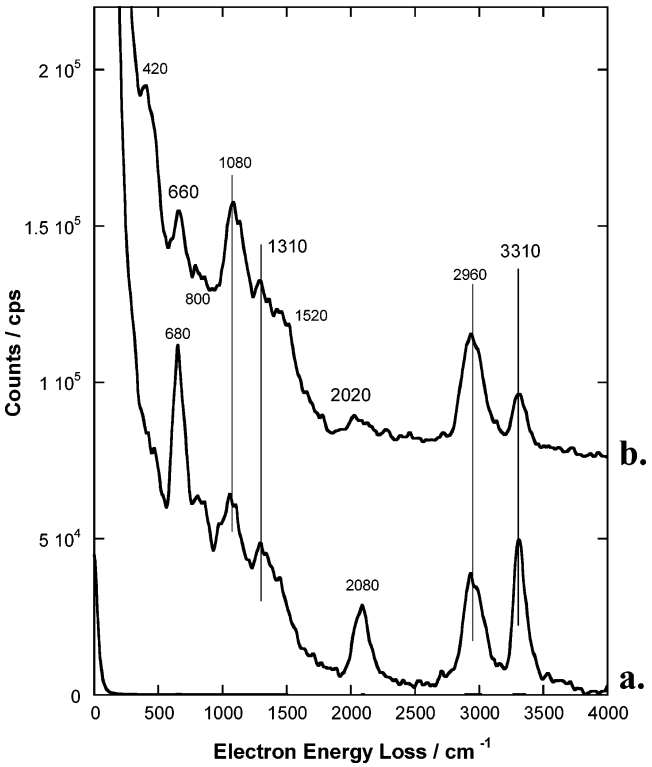

Figure 8. HREELS of H:Si(111) and D:Si(111) treated in 0.5 M CH≡CMgBr/THF at 60 °C solution temperature for 300 min: (a) H:Si(111) after the Grignard reaction and rinsing in 1% CF_3COOH/THF, H_2O, and $CHCl_2CH_2Cl$, ×500 (AES atomic C/Si ratio = 0.55);and (b) D:Si(111) after the Grignard reaction and rinsing in 1% CF_3COOH/THF, H_2O, and $CHCl_2CH_2Cl$, ×1000.

the intensities of D−Si signals. This C≡C stretching frequency is in good agreement with real IR spectra of acetylene, as shown in Table 1. On curve a, the C≡C signal is merged with the H−Si stretching signal, resulting in a relatively high peak. Similarly, the peak at 660 cm^{-1} is also isolated on D:Si(111). This peak is assigned to the stretching motion of the C−Si bond fixing the ethynyl moiety according to Table 1. The two C(1)≡C(2)−H bending normal modes are also anticipated near 660 cm^{-1} and might be contributing to this peak.

The impurity hydrocarbons do not bother this assignment for −C≡C−H modes. In Figure 8, the 2960 cm^{-1} signal is considered to come from longer hydrocarbons. CH_3− directly bonded to Si is excluded, since the Si−CH_3 umbrella mode expected at 1250 cm^{-1} (refs 26 and 28) is not clear. The peak at 1310 cm^{-1} matches the umbrella motion of CH_3 at the end of long alkyl moieties.[40] The continuous background raise from 900 to 1500 cm^{-1} is due to the various CH_2 bending modes in saturated hydrocarbons. The C−Si signals for the alkyls from C_2H_5−[43,44,46] to C_4H_9−[30] are located below 600 cm^{-1}. Therefore, the peak at 660 cm^{-1} is free from the contaminants. Figure 8b recorded for D:Si(111) indicates that the saturated hydrocarbons were not formed mainly by the reaction between −C≡CH groups and surface-terminating hydrogen. The product signal of C−D stretching expected at ∼2100 cm^{-1} is not clear. We may be able to seize the deposition of contaminating hydrocarbon by changing the solvents or the procedure to synthesize the ethynyl Grignard reagent.

The signal at 1080 cm^{-1} is due to SiO_2 impurity, as no modes for adsorbates are predicted for ethynyl groups in Table 1. The small peak at 800 cm^{-1} is a part of the SiO_2 spectrum.[39] The SiO_2 signal significantly bothers the spectra; however, the real amount of SiO_2 in Figure 8 was estimated to be about 7×10^{-3} monolayers.[26] Although the impurities were not rejected, the grafted ethynyl groups are lucid in the spectra, and the ethynyl moieties can be subjected to following reactions at the C≡C sites.

5. Conclusion

Allyl groups, 2-butenyl groups, and ethynyl groups were bonded to surface atoms of Si with the C=C bond or C≡C bond reserved by treating H:Si(111) in the corresponding Grignard reagents. The adsorbates were distributed among H-terminated Si sites, and each of the adsorbates is covalently fixed by a C−Si single bond. The Grignard grafting reaction is considered to proceed mainly just over one single site of Si without temporarily bonding the MgX (X = halogen) species on a vicinal Si site or by breaking the Si−Si back-bond.

The allyl adlayer was almost pure with all bonds reserved after the reaction in the Grignard reagent solution at 45 °C for 5 min. Notably, the terminal C(2)H=C(3)H_2 double bond was preserved. The reaction on H:Si(111) in the 2-butenylmagnesium chloride solution delivered 2-butenyl groups up to 20% of a monolayer. The C=C double bond in the middle of the moiety was stable in the reaction up to 60 °C. Ethynyl moieties were deposited in a CH≡CMgBr/THF solution with a significant amount of saturated hydrocarbons coexisting. The characteristic vibrational signals for ethynyl were well isolated and easily recognized.

The treatment of H:Si(111) in CH_2=CHMgCl/THF resulted in rapid deposition of hydrocarbon moieties mainly composed of CH_2 groups. The double bonds were diminished presumably by further reactions with H:Si(111) and/or the neighboring adsorbates.

The unsaturated hydrocarbon adspecies can be subjected to further organic reactions to add reagents breaking into the double/triple bonds to produce a variety of functional groups, which are applicable to exert chemical functionality and biochemical utility on silicon wafers on the microscopic level.

Acknowledgment. The authors are thankful to the everlasting collaboration with Mr. Tomoyuki Inoue, Dr. Daisuke Niwa, Professor Takayuki Homma, and Professor Tetsuya Osaka at the School of Science and Engineering, Waseda University. We appreciate the computational assistance made by Super Combined Cluster of Advanced Center for Computing and Communication of RIKEN (RSCC).

References and Notes

(1) Whelan, C. S.; Lercel, M. J.; Craighead, H. G.; Seshadri, K.; Allara, D. L. *J. Vac. Sci. Technol.* **1996**, *B14*, 4085.

(2) Sugimura, H.; Okiguchi, K.; Nakagiri, N.; Miyashita, M. *J. Vac. Sci. Technol. B* **1996**, *B14*, 4140.

(3) Yamada, T.; Takano, N.; Yamada, K.; Yoshitomi, S.; Inoue, T.; Osaka, T. *Electrochem. Commun.* **2001**, *3*, 67.

(4) Yamada, T.; Takano, N.; Yamada, K.; Yoshitomi, S.; Inoue, T.; Osaka, T. *Jpn. J. Appl. Phys.* **2001**, *40*, 4845.

(5) Yamada, T.; Takano, N.; Yamada, K.; Yoshitomi, S.; Inoue, T.; Osaka, T. *Mater. Phys. Mech.* **2001**, *4*, 67.

(6) Yamada, T.; Takano, N.; Yamada, K.; Yoshitomi, S.; Inoue, T.; Osaka, T. J. *Electroanal. Chem.* **2002**, *532*, 247.

(7) Harnett, C. K.; Satyalakshmi, K. M.; Craighead, H. G. *Appl. Phys. Lett.* **2000**, *76*, 2466.

(8) Livache, T.; Bazin, H.; Mathis, G. *Clin. Chim. Acta* **1998**, *278*, 171.

(9) Ostroff, R. M.; Hopkins, D.; Haeberli, A. B.; Baouchi, W.; Polisky, B. *Clin. Chem.* **1999**, *45*, 1659.

(10) Lenigk, R.; Carles, M.; Ip, N. Y.; Sucher, N. J. *Langmuir* **2001**, *17*, 2497.

(11) Bennewitz, R.; Crain, R. N.; Kirakosian, A.; Lin, J. L.; McChesney, J. L.; Petrovykh, D. Y.; Himpsel, F. J. *Nanotechnology* **2002**, *13*, 499.

(12) Linford, M. R.; Fenter, P.; Eisenberger, P. M.; Chidsey, C. E. D. *J. Am. Chem. Soc.* **1995**, *117*, 2145.
(13) Quayum, M. E.; Kondo, T.; Nihonyanagi, S.; Miyamoto, D.; Uosaki, K. *Chem. Lett.* **2002**, 208.
(14) Uosaki, K.; Quayum, M. E.; Nihonyanagi, S.; Kondo, T. *Langmuir* **2004**, *20*, 1207.
(15) Nihonyanagi, S.; Miyamoto, D.; Idojiri, S.; Uosaki, K. *J. Am. Chem. Soc.* **2004**, *126*, 7034.
(16) Sieval, A. B.; Demirel, A. L.; Nissink, J. W. M.; Linford, M. R.; Van der Maas, J. H.; De Jeu, W. H.; Zuilhof, H.; Sudhölter, E. J. R. *Langmuir* **1998**, *14*, 1759.
(17) Sieval, A. B.; Vleeming, V.; Zuilhof, H.; Sudhölter, E. J. R. *Langmuir* **1999**, *15*, 8288.
(18) Sieval, A. B.; Lanke, R.; Heij, G.; Meijer, G.; Zuilhof, H.; Sudhölter, E. J. R. *Langmuir* **2001**, *17*, 7554.
(19) Yamada, R.; Ara, M.; Tada, H. *Chem. Lett.* **2004**, *33*, 492.
(20) Ishibashi, T.; Ara, M.; Tada, H.; Onishi, H. *Chem. Phys. Lett.* **2003**, *367*, 376.
(21) Cicero, R. L.; Linford, M. R.; Chidsey, C. E. D. *Langmuir* **2000**, *16*, 5688.
(22) Buriak, J. M. *Chem. Commun.* **1999**, 1051.
(23) Song, J. H.; Sailor, M. J. *J. Am. Chem. Soc.* **1998**, *120*, 2376.
(24) Kim, N. Y.; Laibinis, P. E. *J. Am. Chem. Soc.* **1998**, *120*, 4516.
(25) Boukherroub, R.; Morin, S.; Bensebaa, F.; Wayner, D. D. M. *Langmuir* **1999**, *15*, 3831.
(26) Yamada, T.; Inoue, T.; Yamada, K.; Takano, N.; Osaka, T.; Harada, H.; Nishiyama, K.; Taniguchi, I. *J. Am. Chem. Soc.* **2003**, *125*, 8039.
(27) Fellah, S.; Boukherroub, R.; Ozanam, F.; Chazalviel, J.-N. *Langmuir* **2004**, *20*, 6359.
(28) Yamada, T.; Kawai, M.; Wawro, A.; Suto, S.; Kasuya, A. *J. Chem. Phys.* **2004**, *121*, 10660.
(29) Schmeltzer, J. M.; Porter, L. A., Jr.; Stewart, M. P.; Buriak, J. M. *Langmuir* **2002**, *18*, 2971.
(30) Yamada T.; Noto, M.; Shirasaka, K.; Kato, H. S.; Kawai, M. *J. Phys. Chem. B*, **2006**, *110*, 6740.
(31) Higashi, G. S.; Chabal, Y. J.; Trucks, G. W.; Raghavachari, K. *Appl. Phys. Lett.* **1990**, *56*, 656.
(32) Fukidome, H.; Matsumura, M.; Komeda, T.; Namba, K.; Nishioka, Y. *Electrochem. Solid State Lett.* **1999**, *2*, 393.
(33) Fukidome, H.; Matsumura, M. *Surf. Sci.* **2000**, *463*, L649.
(34) Delley, B. *J. Chem. Phys.* **1990**, *92*, 508.
(35) Delley, B. *J. Phys. Chem.* **1996**, *100*, 6107.
(36) Delley, B. *J. Chem. Phys.* **2000**, *113*, 7756.
(37) Perdew, J. P.; Burke, K.; Ernzerhof, M. *Phys. Rev. Lett.* **1996**, *77*, 3685.
(38) Perdew, J. P.; Burke, K.; Ernzerhof, M. *Phys. Rev. Lett.* **1997**, *78*, 1396.
(39) Shimanouchi, T. *Tables of Molecular Vibrational Frequencies, Consolidated*; National Standard Reference Data Series; National Bureau of Standards: Washington, DC, 1972; Vol. I, p 39.
(40) Coblentz Society, Inc., Evaluated Infrared Reference Spectra. In *NIST Chemistry WebBook*; NIST Standard Reference Database No. 69; Linstrom, P. J. Mallard, W. G., Eds.; NIST: Gaithersburg, MD, 2003 (http://webbook.nist.gov).
(41) Bellamy, L. J. *The infrared spectra of complex molecules*, 3rd ed.; Chapman & Hall: New York, 1975.
(42) Bellamy, L. J. *The infrared spectra of complex molecules*; Advances in Infrared Group Frequencies, 2nd ed.; Chapman & Hall: New York, 1980; Vol. 2.
(43) Bansal, A.; Li, X. L.; Lauermann, I.; Lewis, N. S.; Yi, S. I.; Weinberg, W. H. *J. Am. Chem. Soc.* **1996**, *118*, 7225.
(44) Bansal, A.; Li, X. L.; Yi, S. I.; Weinberg, W. H. *J. Phys. Chem.* **2001**, *B105*, 10266.
(45) Steininger, H.; Ibach, H.; Lehwald, S. *Surf. Sci.* **1998**, *117*, 685.
(46) Nishiyama, K.; Tanaka, Y.; Harada, H.; Yamada, T.; Niwa, D.; Inoue, T.; Homma, T.; Osaka, T.; Taniguchi, I., *Surf. Sci.* In press.
(47) Grégoire, C.; Yu, L. M.; Bodino, F.; Tronc, M.; Pireaux, J. J. *J. Electron Spectrosc. Relat. Phenom.* **1999**, *98/99*, 67.